PHYSICAL REVIEW E **96**, 030901(R) (2017)

Friction force regimes and the conditions for endless penetration of an intruder into a granular medium

L. A. López-Rodríguez and F. Pacheco-Vázquez*

Instituto de Física, Benemérita Universidad Autónoma de Puebla, Apartado Postal J-48, Puebla 72570, Mexico

(Received 7 June 2017; published 25 September 2017)

An intruder penetrating into a granular column experiences a depth-dependent friction force $F(z)$. Different regimes of $F(z)$ have been measured depending on the experimental design: a nearly linear dependence for shallow penetrations, total saturation at large depths, and an exponential increase when the intruder approaches the bottom of the granular bed. We report here an experiment that allows us to measure the different regimes in a single run during the quasistatic descent of a sphere in a light granular medium. From the analysis of the resistance in the saturation zone, it was found that $F(z)$ follows a cube-power-law dependence on the intruder diameter and an exponential increase with the packing fraction of the bed. Moreover, we determine the critical mass m_c required to observe infinite penetration and its dependence on the above parameters. Finally, we use our results to estimate the final penetration depth reached by intruders of masses $m < m_c$. The results indicate that an intruder of any density (larger than the density of the granular bed) can sink indefinitely into the granular medium if the bed packing fraction is smaller than a critical value.

DOI: 10.1103/PhysRevE.96.030901

I. INTRODUCTION

Since the 19th century, the penetration dynamics of projectiles in sand and clay was already an important topic in ballistics [1]. Initial experiments were focused on the resistance force to horizontal penetration at low velocities ($v < 100$ m/s) [2–5]. Poncelet [3] posed a total resistance given by the sum of two terms: a constant friction term plus a viscous term, similar to that in fluids, proportional to the velocity square. At the beginning of the present century, the understanding of impact cratering motivated laboratory-scale studies about the impact and vertical penetration of projectiles in a model granular bed [6–11]. In this context, the dynamics of a projectile of mass m falling through a granular medium under the influence of gravity g is well approached by the expression

$$m\ddot{z} = mg - F(z) - \eta\dot{z}^2, \tag{1}$$

where $F(z)$ is a friction term, often taken to be linear with depth z [10,11], and η is a constant. More recent studies propose the addition of a term linear in velocity to the viscous drag [12,13], or a linear differential equation based on energy-depth analysis [14]. It was also reported that the frictional term scales as the square root of the density of the granular medium and projectile, which is typically larger than the combination of hydrostatic pressure and Coulomb friction law [15]. Nevertheless, in Ref. [16], it was shown that $F(z)$ is determined by the normal force proportional to the intruder surface. This force is set by a friction coefficient, hydrostatic pressure, and the projectile size and shape. The linear dependence on depth is only recovered for spherical projectiles when z is larger than the ball diameter [16,17].

On the other hand, the friction term $F(z)$ becomes constant if a projectile penetrates very deep into a granular column until reaching the zone where the pressure saturates due to the Janssen effect [8,18,19]. This happens if the projectile density is much larger than the density of the confined grains [19], or, as we show in the present work, for low packing fractions of the bed. Under these considerations, the projectile motion is well described by

$$m\ddot{z} = mg - \kappa\lambda(1 - e^{-z/\lambda}) - \eta\dot{z}^2, \tag{2}$$

where κ is a constant, and λ is a saturation length [19]. Finally, when the projectile is getting to the bottom of the column, the resistance force increases exponentially as $F(z) \propto e^{-z/\delta}$, where δ is a characteristic length scale for sensing the bottom of the container [8].

In this Rapid Communication, the different regimes of the static friction term are detected by directly measuring $F(z)$ using a force sensor while the intruder penetrates a column of expanded polystyrene beads. In contrast to Refs. [18–20], the experiments were performed at a negligible velocity in order to discard the inertial viscous term. Our work is focused mainly on two aspects: (a) to measure the transition between different regimes and describe the dynamics with a single equation for $F(z)$, and (b) to explore the effect of intruder size and packing fraction (the latter rarely analyzed; see, e.g., Ref. [13]) in the final penetration depth.

II. EXPERIMENTAL SETUP

The experimental setup is sketched in Fig. 1(a). The silo consists of a cardboard tube of inner diameter $D_{\text{silo}} = 35.3 \pm 0.05$ and 300 cm long filled with 3360 ± 1 g of expanded polystyrene beads (average density $\rho_g = 0.022$ g/cm^3 and radius $r = 2 \pm 0.5$ mm). The effective density of the granular bed obtained when the material was poured from the top is $\rho_{\text{eff}} = 0.0128$ g/cm^3 [see Fig. 1(b)], which allows us to calculate the bed packing fraction $\phi_{\text{poured}} = \rho_{\text{eff}}/\rho_g = 0.582 \pm 0.001$. The intruders consisted of hollow polyurethane balls of diameters d_b ranging from 3.0 to 9.4 ± 0.1 cm filled with different amounts of lead to obtain masses m between 50 and 1076 ± 1 g. Solid lead balls were also used, and in all cases, the intruders were covered with a thin layer of latex to obtain the same surface roughness. A ball of a selected mass is hung

*Corresponding author: fpacheco@ifuap.buap.mx

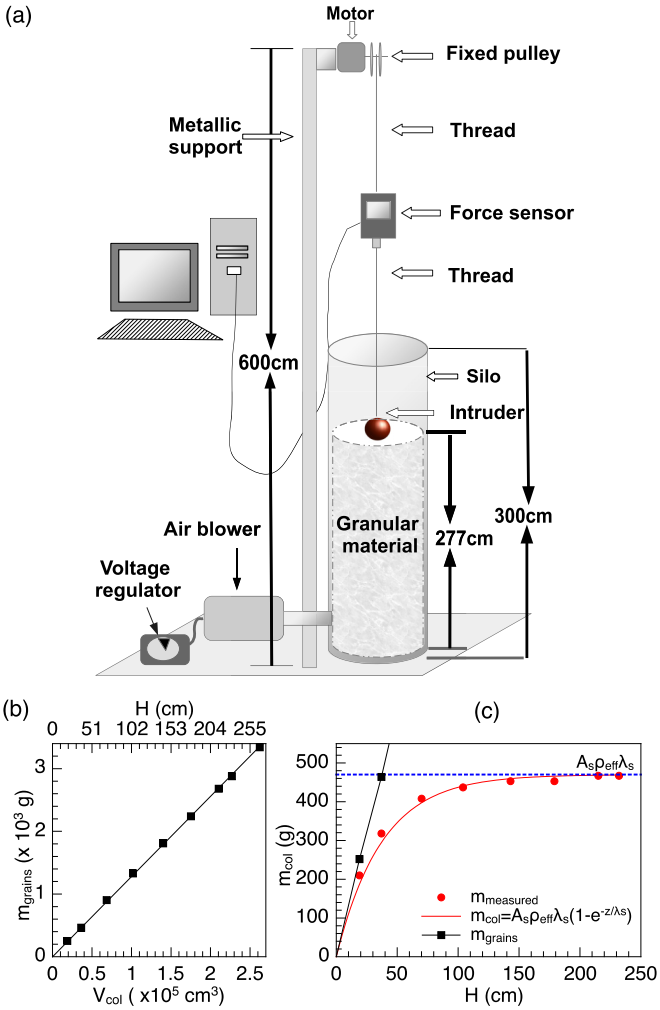

FIG. 1. (a) Sketch of the experimental setup: A long silo filled with light grains is slowly penetrated by an intruder. The drag force is monitored using a digital force gauge. (b) Mass of grains poured into the silo vs column height H or vs equivalent occupied volume $V_{\rm col}$; the black line slope gives the effective density of the bed ($\rho_{\rm eff} = 0.0128$ g/cm^3). (c) The mass of the granular column m, measured at the bottom of the silo, as a function of H, follows a Janssen-like dependence (red line). Mass saturation (dashed blue line) allows us to estimate the saturation length $\lambda_s \sim 38$ cm for the static bed.

with a 3 m fine thread from a force gauge Omega DFG35-5 suspended beneath a pulley connected to a dc geared motor fixed at a height of 6 m from the bottom of the silo. This array allows the intruder to descend through the granular medium at a constant velocity and measure its apparent weight without interference on the force gauge, which never enters into the bed.

Before each penetration, the material is prepared to a reproducible loose random packing by slowly turning off a fluidizing upflow of air injected with an air pump connected at the bottom of the container, which leaves a column of 277 ± 0.5 cm high with a packing fraction $\phi = 0.566 \pm 0.001$ when the air flow has been totally suppressed. Subsequently, ϕ is increased in the range $0.566 < \phi < 0.613$ by tapping uniformly the silo wall. The change in packing is measured by a noticeable shift of the granular surface level (0–21 cm). Once

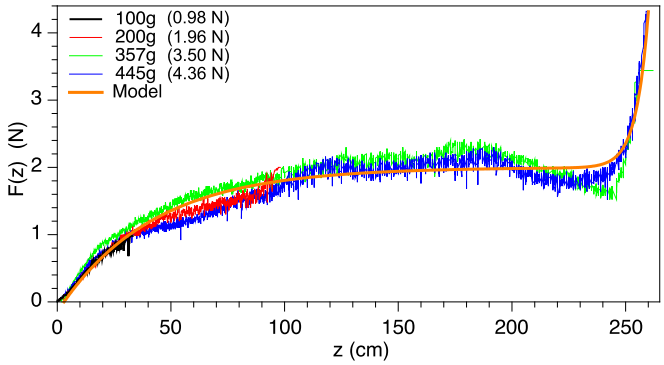

FIG. 2. F vs z during the penetration of spherical intruders of different masses and constant diameter, $d_b = 5.4$ cm, into a light granular column with packing fraction $\phi = 0.566$.

the granular column is ready, the ball is located at the surface of the bed, the force gauge is started, and the motor is turned on to start the descent at a constant velocity $v_c = 1.1 \pm 0.05$ cm/s while the data are captured at 10 Hz with an accuracy of ± 0.01 N. Initially, the force gauge indicates the intruder weight $W = mg$ because the ball hangs freely. Then, the gauge is set to zero to obtain directly the depth-dependent resistance F_d. As the ball penetrates into the bed, the reading increases until it reaches $F_d = W$, when the intruder stops sinking at a final depth $Z_{\rm f}$, or a constant value $F_d < W$, when the intruder reaches the saturation zone. The force gauge measures F_d versus time t, and it is converted to F_d versus depth z by simply using $z = v_c t$. After one run, the bed is prepared again and the procedure is repeated five times for several masses, diameters, and packings in the ranges indicated above.

III. RESULTS AND DISCUSSION

A. Different regimes of $F(z)$

Figure 2 shows the resistance F as a function of z for intruders of different masses penetrating into the loosely packed medium ($\phi = 0.566$). For $m = 100$ g, $F(z)$ increases nearly linearly until the ball stops at $z \approx 30$ cm when $F(z) = W \approx 0.98$ N. For $m = 200$ g, $F(z)$ increases and starts to saturate with z, but the intruder still stops at a finite depth ($\sim$100 cm) when $F(z) \approx 1.96$ N.

A complete saturation of the resistance force is observed for $m = 357$ and 445 g. Note that the plateau is reached about $F(z) \approx 2$ N. This saturation force $F_{\rm sat}$ is smaller than the required force to stop the intruders (3.5 and 4.36 N, respectively). Deeper, an exponential growth of $F(z)$ is observed when the balls approach the bottom of the silo, and they stop when $F(z) = W$ in each case. In principle, these spheres would sink indefinitely in an infinite silo. It is important to mention that the noise present in the measurements is because force chains extend from the intruder deep into the medium and are intermittently loaded and broken during the intruder passage [21]. These force chain fluctuations are of the order of 0.3 N. On the other hand, the oscillations of $F(z)$ eventually observed in the saturation zone are related to an inhomogeneous packing fraction produced during the bed preparation process.

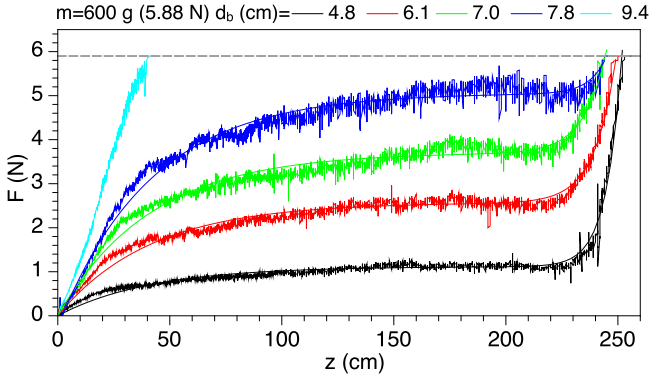

FIG. 3. F vs z during the penetration of a spherical intruder of constant mass and different diameters. The packing fraction of the bed is also constant, $\phi = 0.566$. In four cases, $F_{\rm sat} < W$, and the intruder reaches the saturation zone.

In order to obtain a single expression for the resistance force as a function of depth, let us consider the saturating term of Eq. (2) describing the friction force in an infinite silo [19], combined with the exponential term for intruders reaching the bottom of a container [8]. The latter term must be negligible for $z \ll H$ where only the saturation term is important, but it must become dominant when z approaches H. Thus, $F(z)$ can be written as

$$F(z) = \kappa\lambda(1 - e^{-(z-z_0)/\lambda}) + Ae^{-(H-z)/\lambda^*}, \qquad (3)$$

where λ is the saturation length, $H = 277$ cm is the height of the granular column, and λ^* is a length related to the confinement effects at the bottom of the silo. The parameter z_0 was introduced by taking into account a nonlinear increase of $F(z)$ at the beginning of the penetration [16,17], which can be neglected for loose packings but becomes important at high packings, as it is shown in Sec. III C. The product $\kappa\lambda = 2.0 \pm 0.1$ N is given by the average of the resistance in the plateau. With the above values, Eq. (3) was used to fit the data for $m = 445$ g in Fig. 2 (orange line), which gives $\lambda = 41.5 \pm 0.1$ cm $\sim O(\lambda_s)$, $\kappa = 0.0482$ N/cm, $\lambda^* \approx 5.4$ cm $\sim O(d_b)$, and $z_0 \sim 3$ cm. Note that $z_0 \ll \lambda$ is negligible for $\phi = 0.566$.

B. Penetration of intruders with different sizes

Figure 3 shows F vs z for an intruder of constant mass $m = 600$ g penetrating into a bed of constant packing $\phi = 0.566$ for different values of d_b: For $d_b \lesssim 7.8$ cm, the intruder reaches the saturation zone, for $d_b = 9.4$ cm, the intruder stops at $z \approx 40$ cm, displaying only the linear regime, but in all cases the penetration finishes at $F = 5.88$ N when the ball weight is equilibrated.

Figure 4(a) shows that the average force in the saturation zone $F_{\rm sat}$ increases with d_b (black squares). The $\log_{10}$ - $\log_{10}$ plot in the inset reveals a power-law dependence given by $F_{\rm sat} = (0.015 \pm 0.002)d_b^{2.83\pm0.08} \approx Ad_b^3$. Since $F_{\rm sat} = \kappa\lambda$, from Eq. (3) one can write the resistance force without considering the bottom effects as

$$F(z) \approx Ad_b^3(1 - e^{-(z-z_0)/\lambda}). \qquad (4)$$

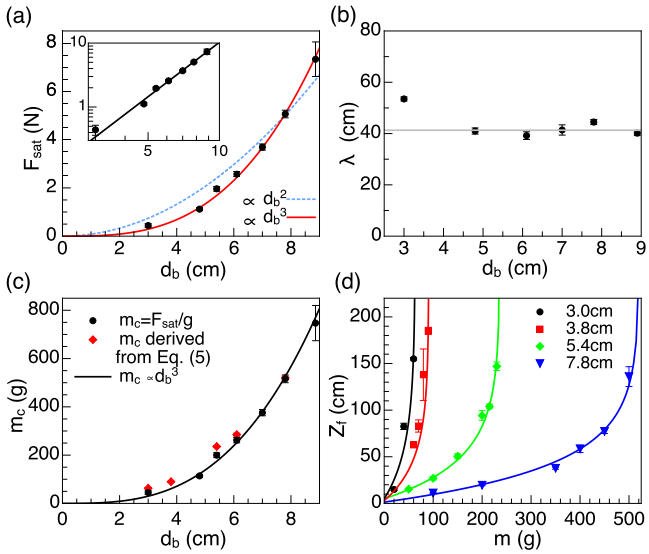

FIG. 4. (a) $F_{\rm sat}$ vs d_b: The experimental data (black symbols) are well described by a cube-power law (red line) as it is confirmed by the log-log plot in the inset. (b) λ vs d_b: The gray line indicates the value $\lambda = 41.5$ cm $\sim \lambda_s$. (c) m_c vs d_b obtained by the two methods described in the text. (d) $Z_{\rm f}$ vs m for four values of d_b. Data are well described by using Eq. (5).

In Ref. [16], it was found that the local friction force during projectile penetration increases with depth according to the expression $d\mathbf{F} = \alpha\mu(\rho g z)d\mathbf{A}$, where μ is an internal friction coefficient, $\rho g z$ is the gravitational loading pressure, $d\mathbf{A}$ is an infinitesimal area element pointing normal to the projectile surface, and α a constant of proportionality. For the spherical case, the above expression predicts $F(z) \propto d_b^2$. Note, however, in Fig. 4(a), that the square-power dependence (dotted blue line) is far from our experimental results, which are better approached by the cube-power dependence described above (red line).

It is important to clarify that the results in Ref. [16] were obtained for shallow depths of the order of one sphere diameter (∼3 cm). Here, we consider deep penetrations where F becomes independent of z, and the effect of d_b was measured directly in a long depth range and far from the bed surface. Moreover, the magnitude of λ can be evaluated by adjusting the curves in Fig. 3 with Eq. (3). The resulting data shown in Fig. 4(b) indicate that $\lambda \sim O(41.5$ cm), largely independent of d_b.

Additionally, we estimated the critical mass m_c required to reach the saturation zone depending on the intruder diameter considering the fact that in this zone, $F_{\rm sat} = m_c g$. The values of m_c vs d_b are shown in Fig. 4(c) (black dots). Another method to find m_c is by varying the mass of an intruder that stops at a final depth $Z_{\rm f}$ until reaching the mass at which the intruder does not stop. This procedure was followed using spheres of several diameters and the results are shown in Fig. 4(d) (symbols). Since $Z_{\rm f}$ is reached when the intruder weight is balanced by $F(z)$, far from the bottom one can write $mg = k\lambda(1 - e^{-(Z_{\rm f}-z_0)/\lambda})$, and solving for $Z_{\rm f}$,

$$Z_{\rm f} = -\lambda \ln(1 - m/m_c) + z_0, \qquad (5)$$

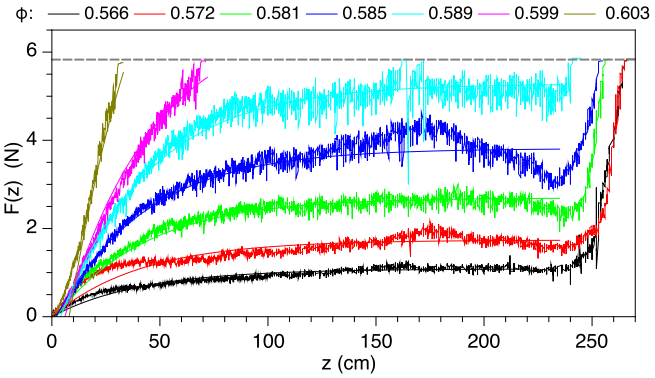

FIG. 5. $F(z)$ vs z experienced by an intruder of constant mass $m = 600$ g ($W = 5.88$ N) and diameter $d_b = 4.8$ cm for different packing fractions. The dashed line corresponds to $F(z) = W$ and the intruder stops when this value is reached.

where $m_c = \kappa\lambda/g$ and z_0 is negligible for loose packing. Equation (5) was used to fit the experimental measurements using $\lambda = 41.5$ cm and leaving m_c as the free parameter. The best fits represented in Fig. 4(d) by solid lines allowed us to obtain the values of m_c vs d_b. The resulting values plotted in Fig. 4(c) as red diamonds are in all cases a bit larger than the values given by the saturation force. Our explanation is that, in the first method, we used the average of the resistance force in the saturation zone $F_{\rm sat}$; however, as it can be noticed from the plots in Fig. 3, there exist fluctuations larger than the mean value able to stop the intruder of $m_c = F_{\rm sat}/g$. Therefore, it is necessary to have a mass value slightly higher than the predicted one to surpass the stronger force chains and penetrate indefinitely the granular column.

C. Effect of packing fraction

Another important parameter that determines the resistance force is the packing fraction of the bed. Figure 5 shows F vs z for an intruder of constant mass ($m = 600$ g, weight $W = 5.88$ N) penetrating into beds with different values of ϕ. For packings $\phi \leqslant 0.589$, the intruder reaches the saturation zone and penetrates deep into the bed until stopping close to the bottom when the force grows exponentially. At higher packings, only the nearly linear regime is observed, the resistance force grows faster, and the intruder stops when its weight is equilibrated by $F(z) = 5.88$ N.

As in the previous case, the average of the saturation force in the plateau was obtained and it was plotted as a function of ϕ in Fig. 6(a). The resulting data show an exponential growth and are well fitted by the equation

$$F_{\rm sat} = \beta d_b^3 \left(e^{\gamma\left(\frac{\phi-\phi_0}{\phi_{\rm max}-\phi}\right)} - 1\right), \qquad (6)$$

where $\beta = 0.042 \pm 0.002$ N, $\gamma = 0.57 \pm 0.06$, $\phi_{\rm max} = 0.620 \pm 0.005$, and $\phi_0 = 0.548$. Here, d_b^3 is introduced based on the previous analysis and in this case $d_b = 4.8$ cm. The parameter ϕ_0 is the packing value at which $F(z)$ acting on the intruder is zero. The value of ϕ_0 was estimated by performing the experiment with the air flow "on" at different flow rates to expand the granular bed. When the grains start to be suspended by the interstitial air flow, the contact among them

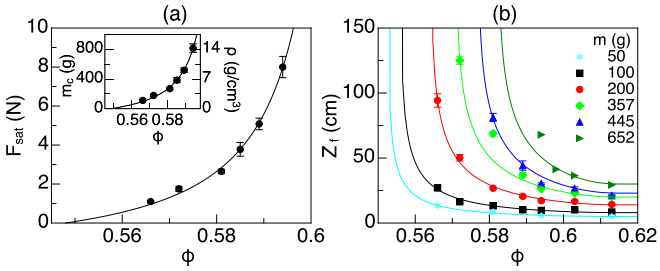

FIG. 6. (a) Main plot: $F_{\rm sat}$ vs ϕ; inset: $m_c = F_{\rm sat}/g$ vs ϕ (points). Black lines correspond to the best fit of the data given by Eq. (6). (b) $Z_{\rm f}$ vs ϕ for intruders of 5.4 cm diameter and different masses. Solid lines correspond to Eq. (8).

is lost and the friction $F(z)$ approaches zero. This happened when $\phi \approx 0.545$–0.548. The best fit of the experimental data, represented in Fig. 6(a) by the black line, is in good agreement with the experimental estimation. It is important to clarify that the air flow was maintained "on" during the experiment only for the case $\phi = \phi_0$. For the rest of the experiments, the air flow was only used to prepare the bed and turned off before the intruder penetration.

Since $F_{\rm sat} = \kappa\lambda$, and given its dependence on d_b and ϕ found above, from Eq. (3), we can write down an expression for $F(z)$ as follows,

$$F(z) \approx \beta d_b^3 \left(e^{\gamma\left(\frac{\phi-\phi_0}{\phi_{\rm max}-\phi}\right)} - 1\right)\left(1 - e^{-(z-z_0)/\lambda}\right). \qquad (7)$$

This equation is plotted in Fig. 5 (overlapping lines) for different values of ϕ using $\lambda = 41.5$ cm and the constant values obtained from Eq. (6). The agreement with the experimental results is remarkable.

One can also estimate the minimum intruder mass required to observe infinite penetration depending on the packing fraction considering that $F_{\rm sat} = m_c g$. The resulting values of m_c vs ϕ are shown in the inset of Fig. 6(a). The right axis indicates the corresponding intruder density. If the bed is prepared at a given packing, an intruder with density above the black line would sink endlessly through the granular bed.

Finally, we measured the final depth $Z_{\rm f}$ reached by an intruder of a given mass depending on the packing fraction of the bed. The experimental data are shown in Fig. 6(b) (symbols). Using $m_c = F_{\rm sat}/g$ and combining Eqs. (5) and (6), one obtains

$$Z_{\rm f} = -\lambda \ln\left(1 - \frac{mg}{\beta d_b^3 \left(e^{\gamma\left(\frac{\phi-\phi_0}{\phi_{\rm max}-\phi}\right)} - 1\right)}\right) + z_0. \qquad (8)$$

This expression is plotted in Fig. 6(b) as a function of ϕ for different values of m (colored lines) with β as the unique free parameter and z_0 determined from the penetration at the maximum packing. The solutions of the equation describe reasonably well the experimental results in the explored range. The exact dependence of the free parameters on the medium properties and intruder geometry was not analyzed in this research, and caution should be used in using their values due to the high sensitivity of the system to the volume fraction. Nevertheless, the existence of the saturation force (i.e., a critical mass) and its dependence on the packing and intruder volume are robust results measured directly during

the penetration, and are important contributions of the present study.

IV. CONCLUSIONS

The depth-dependent resistance to the penetration of a spherical intruder into an ultralight granular column was analyzed by varying the intruder diameter, its mass, and packing fraction of the medium in an environment that allows one to neglect the inertial drag contribution. The results confirm that, under specific conditions, an intruder can penetrate indefinitely through a granular column due to the Janssen-like saturation of the friction force. The most remarkable result is that this force is proportional to the sphere volume, which is in contrast with the square-law dependence of $F(z)$ reported previously for shallow penetrations [16]. Moreover, the resistance force and hence the critical mass to observe infinite penetration grow exponentially with the packing fraction of the bed. Our findings show that the parametric window to observe such a rare event is very reduced, and that is the reason why the reported dynamics is not commonly found in nature. Nonetheless, infinite penetration could probably be observed with dense projectiles falling into dry quicksand or through granular media totally immersed in a liquid, where the effective density of the granular bed is reduced by buoyant forces.

ACKNOWLEDGMENTS

This research was supported by CONACyT Mexico Project No. 242085 of the Sectoral Research Fund for Education, and VIEP-BUAP 2017. L.A.L.R. thanks CONACyT Mexico for supporting her studies through a Master degree scholarship.

[1] H. P. Robertson, *Terminal Ballistics* (National Research Council, Washington, D.C., 1941).
[2] B. Robins, *New Principles of Gunnery* (Wright, London, 1742).
[3] J. V. Poncelet, *Cours de Mécanique Industrielle*, 1st ed. (Recknagel, Bruxelles, 1829).
[4] M. H. Résal, Compt. Rend. (Paris) **120**, 397 (1895).
[5] W. A. Allen, E. B. Mayfield, and H. L. Morrison, J. Appl. Phys. **28**, 370 (1957).
[6] M. P. Ciamarra, A. H. Lara, A. T. Lee, D. I. Goldman, I. Vishik, and H. L. Swinney, Phys. Rev. Lett. **92**, 194301 (2004).
[7] J. R. de Bruyn and A. M. Walsh, Can. J. Phys. **82**, 439 (2004).
[8] M. B. Stone, D. P. Bernstein, R. Barry, M. D. Pelc, Y. K. Tsui, and P. Schiffer, Nature (London) **427**, 503 (2004).
[9] L. S. Tsimring and D. Volfson, *Powders and Grains* (A. A. Balkema, Rotterdam, 2005).
[10] D. Lohse, R. Rauhé, R. Bergmann, and D. van der Meer, Nature (London) **432**, 689 (2004).
[11] H. Katsuragi and D. J. Durian, Nat. Phys. **3**, 420 (2007).
[12] D. I. Goldman and P. B. Umbanhowar, Phys. Rev. E **77**, 021308 (2008).
[13] P. B. Umbanhowar and D. I. Goldman, Phys. Rev. E **82**, 010301 (2010).
[14] A. H. Clark and R. P. Behringer, Europhys. Lett. **101**, 64001 (2013).
[15] H. Katsuragi and D. J. Durian, Phys. Rev. E **87**, 052208 (2013).
[16] T. A. Brzinski, P. Mayor, and D. J. Durian, Phys. Rev. Lett. **111**, 168002 (2013).
[17] Z. Peng, X. Xu, K. Lu, and M. Hou, Phys. Rev. E **80**, 021301 (2009).
[18] F. Pacheco-Vázquez and J. C. Ruiz-Suárez, Phys. Rev. E **80**, 060301(R) (2009); Nat. Commun. **1**, 123 (2010).
[19] F. Pacheco-Vázquez *et al.*, Phys. Rev. Lett. **106**, 218001 (2011).
[20] E. Altshuler *et al.*, Geophys. Res. Lett. **41**, 3032 (2014).
[21] A. H. Clark, L. Kondic, and R. P. Behringer, Phys. Rev. Lett. **109**, 238302 (2012).